Carbohydrate Polymers 176 (2017) 195–202

Contents lists available at ScienceDirect

Carbohydrate Polymers

journal homepage: www.elsevier.com/locate/carbpol

Research Paper

Design and fabrication of a chitosan hydrogel with gradient structures via a step-by-step cross-linking process

Yongxiang Xu[a,b,c,1], Shenpo Yuan[a,b,c,1], Jianmin Han[a,b,c,1], Hong Lin[a,b,c,*], Xuehui Zhang[a,b,c,*]

[a] Department of Dental Materials, Peking University School and Hospital of Stomatology, Beijing 100081, China
[b] National Engineering Laboratory for Digital and Material Technology of Stomatology, Beijing 100081, China
[c] Beijing Key Laboratory of Digital Stomatology, Beijing 100081, China

ARTICLE INFO

Article history:
Received 3 February 2017
Received in revised form 31 July 2017
Accepted 7 August 2017
Available online 23 August 2017

Keywords:
Chitosan
Hydrogel
Gradient structure
Step-by-step cross-linking

ABSTRACT

The development of scaffolds to mimic the gradient structure of natural tissue is an important consideration for effective tissue engineering. In the present study, a physical cross-linking chitosan hydrogel with gradient structures was fabricated via a step-by-step cross-linking process using sodium tripolyphosphate and sodium hydroxide as sequential cross-linkers. Chitosan hydrogels with different structures (single, double, and triple layers) were prepared by modifying the gelling process. The properties of the hydrogels were further adjusted by varying the gelling conditions, such as gelling time, pH, and composition of the crosslinking solution. Slight cytotoxicity was showed in MTT assay for hydrogels with uncross-linking chitosan solution and non-cytotoxicity was showed for other hydrogels. The results suggest that step-by-step cross-linking represents a practicable method to fabricate scaffolds with gradient structures.

1. Introduction

The developing field of tissue engineering aims to regenerate damaged tissues by combining cells from the body with highly porous scaffold biomaterials, which act as templates for tissue regeneration (O'Brien, 2011). One of the challenges in the development of such scaffolds is to adequately mimic the gradient structure of natural tissue such as bone, cartilage, tooth, skin, and vessels (Levingstone, Matsiko, Dickson, O'Brien, & Gleeson, 2014). Systems with gradients in material composition, bioactive signals, or substrate modulus have been widely explored for different applications including protein delivery systems, directing neuronal growth, investigating cell-microenvironment interactions, enhancing cell proliferation, and for interfacial tissue engineering (Chatterjee, Sun, Chow, Young, & Simon, 2010; Mohan et al., 2011; Seidi, Ramalingam, Elloumi-Hannachi, Ostrovidov, & Khademhosseini, 2011).

In particular, hydrogels, which comprise insoluble hydrophilic polymer networks formed through the gelling of water-soluble polymers, have found widespread application in tissue engineering as their aqueous, structured environment may partially mimic the natural extracellular matrix (Geckil, Xu, Zhang, Moon, & Demirci, 2010; Slaughter, Khurshid, Fisher, Khademhosseini, & Peppas, 2009). Hydrogels also represent attractive scaffolds for controlling cell function, as a variety of technologies and chemistries have been developed for tailoring their biochemical and physical properties (Burdick, Chung, & Jia, 2005). Generally, the methods used to modulate hydrogel properties typically result in isotropic properties because the gels are created from homogeneously mixed solutions. Alternatively, hydrogels with gradients in biosignals, composition, and structure have been fabricated in recent years by freezing-thawing (Kim et al., 2015), gradient polymerization (Karpiak, Ner, & Almutairi, 2012; Tan et al., 2015), 3D printing (Sobral, Caridade, Rui, Mano, & Rui, 2011), and microfluidics (Mahadik, Wheeler, Skertich, Kenis, & Harley, 2014; Pedron, Becka, & Harley, 2015) methodologies. However, these systems often employ long and sophisticated fabrication procedures that necessitate expertise and expensive equipment (Jeon, Alt, Linderman, & Alsberg, 2013; Karpiak et al., 2012).

* Corresponding authors at: Department of Dental Materials, Peking University School and Hospital of Stomatology, Beijing 100081, China.
E-mail addresses: xuyx@hsc.pku.edu.cn (Y. Xu), yuanshenpo@163.com (S. Yuan), hanjianmin@bjmu.edu.cn (J. Han), hong196lin@sina.com (H. Lin), zhangxuehui914@163.com (X. Zhang).
[1] Department of Dental Materials, Peking University School and Hospital of Stomatology, Beijing 100081, China.

http://dx.doi.org/10.1016/j.carbpol.2017.08.032
0144-8617/

Chitosan, a compound derived from the partial deacetylation of natural chitin, consists of a linear, semi-crystalline polysaccharide that exhibits many desirable intrinsic properties such as biocompatibility, biodegradability, and sterilization, which make it an outstanding candidate for biomedical applications (Bhattarai, Gunn, & Zhang, 2010; Domard, 2011; Sashiwa & Aiba, 2004; Silva, Juenet, Meddahi-Pellé, & Letourneur, 2015; Zhang et al., 2012). Accordingly, chitosan hydrogels including thermosensitive hydrogels and micro/nanogels, represent the most widely used biomaterials for drug delivery, gene delivery, and tissue engineering (Abd-Allah, Kamel, & Sammour, 2016; Hui, Ling, Pei, Li, & Xi, 2015). Notably, the primary aliphatic amines ($pKa = 6.3$) of chitosan may be protonated under acidic conditions, which renders the molecule fully soluble (Bhattarai et al., 2010). Consequently, the chitosan solution forms entangle physical gels via secondary interactions (Van der Waals interactions and hydrogen bonds) resulting from the increase in pH (Berger, Reist, Mayer, Felt, & Gurny, 2004; Domard, 2011; Ho et al., 2004; Hsieh et al., 2007; Silva et al., 2015). Multilayered bulk hydrogels are fabricated by exploiting the pH-dependent solubility of chitosan through periodic neutralization of the chitosan solution with NaOH (Dash, Chiellini, Ottenbrite, & Chiellini, 2011; Ladet, David, & Domard, 2008; Montembault, Viton, & Domard, 2005). Furthermore, tripolyphosphate (TPP) has often been used as an ionic gelling agent to prepare chitosan beads, gels, nanoparticles, and films owing to its non-toxic properties and gelling ability and stability in acid environments (Anitha et al., 2011; Jin, Zeng, Liu, & He, 2013; Rampino, Borgogna, Blasi, Bellich & Cesàro, 2013). Together, for example, these techniques have allowed the successful preparation of biomimetic multi-layered hollow chitosan-TPP hydrogel rods in NaOH solution by semipermeable membrane (Nie, Wang, Zhang, & Hu, 2015).

As a result, fabrication of physical chitosan hydrogels with the same gradient structure as human tissues was one of important research topic. By now, more literatures focused on the preparation methods on nano/micro gels, fibers and films of chitosan (Agnihotri, Mallikarjuna, & Aminabhavi, 2004). The methods for bulk chitosan hydrogels such as lyophilization and neutralization were difficult to control the gradient structure (Levengood & Zhang, 2014). The current study aimed to fabricate a chitosan-based physical gradient hydrogel via a step-by-step gelation by TPP and NaOH in sequence with assistant of NaCl. The influence of the preparation conditions on hydrogel structure and properties were further examined.

2. Material and methods

2.1. Materials

Chitosan ($M_w = 187$ kDa, degree of de-acetylation = 89.8%) was purchased from Beijing HWRK Chem Co., Ltd., China and purified before use. Acetic acid (CH_3COOH), NH_4OH, bromothymol blue, phosphate buffer saline ($1 \times$ PBS), sodium acetate (CH_3COONa), sodium chloride (NaCl), and sodium hydroxide (NaOH) were purchased from Sinopharm Chemical Reagent Beijing Co., Ltd., China. TPP was purchased from Sigma-Aldrich Co., Germany. All chemicals were analytical grade and used without further purification.

2.2. Purification and characterization of chitosan

Briefly, a chitosan solution was prepared in CH_3COOH aqueous solution and sequentially filtered through membranes. The filtrate was precipitated with dilute NH_4OH and centrifuged, then repeatedly rinsed with de-ionized water and centrifuged until a neutral pH was achieved before dispersion in water and freeze-drying.

The average viscosimetric molecular weight ($\bar{M}_\eta$) of chitosan was 187 kDa, as determined using an Ubbelohde viscometer with the Mark-Houwink-Sakurada equation: $[\eta] = 0.0843\bar{M}_\eta^{0.78}$. The degree of de-acetylation of the chitosan was 89.8%, as measured by ATR-FTIR spectroscopy using a Nicolet iN10 spectrometer (Thermo Scientific, Waltham, MA, USA) (Brugnerotto et al., 2001).

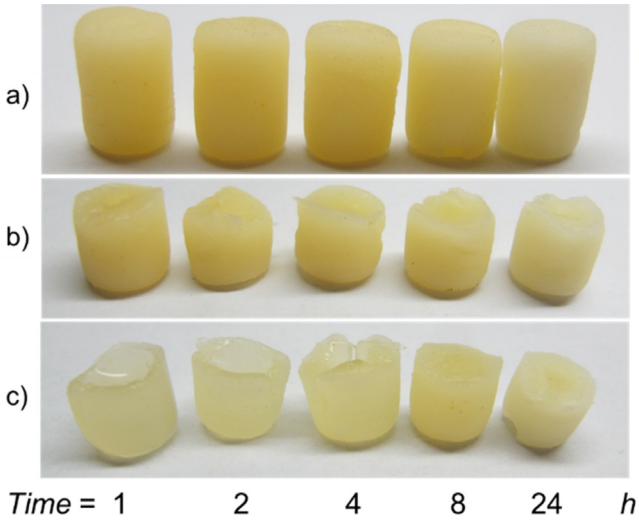

Fig. 1. Digital images showing the chitosan hydrogel formed in the first gelling solution (3 M NaCl + 0.5% TPP, $pH = 5.0$) at different times (1, 2, 4, 8, and 24 h). a) Cylindrical hydrogel; b) Hydrogels after being cut in half; c) hydrogels following through washing with de-ionized water after being halved. Bromothymol blue (pH = 6.0–7.6, yellow to blue) was added as a pH indicator for visibility. (For interpretation of the references to colour in this figure legend, the reader is referred to the web version of this article.)

2.3. Preparation of chitosan hydrogels

Chitosan was dispersed in de-ionized water and a stoichiometrically equivalent amount of acetic acid was added. After complete dissolution, the solution was left to stand for 24 h without stirring for degassing at 4 °C. The solution was then injected into a cylindrical mold and frozen at −20 °C for 24 h. The frozen chitosan was immersed in the first gelling solution (NaCl + TPP) at 4 °C for various times. The hydrogel was then further treated by a second gelling solution (NaOH). Finally, all the samples were washed three times with de-ionized water (or $1 \times$ PBS, pH = 7.4) and then stored in it for 24 h before testing. As comparison, the hydrogels were also prepared by TPP, NaCl + TPP, NaOH and NaCl + NaOH, separately.

2.4. Gelation of chitosan hydrogels

To examine the gelation process, bromothymol blue was added to the chitosan solution as an indicator (pH = 6.0–7.6, yellow to blue). Briefly, one sample was removed from the gelling solution at each time point and then cut in half to observe the morphology and color of the whole sample. The thickness of the gel layer (blue) was measured after washing thoroughly with de-ionized water to remove the inside uncross-linked chitosan solution (yellow). The gelation rate was determined as the ratio between the thickness of the gel layer and the gelling time.

2.5. Structure of chitosan hydrogels

Images of hydrogels forming under various conditions were captured using a digital camera (EOS 5D Mark II, Canon, Tokyo, Japan). Furthermore, the liquid-nitrogen fracture surfaces of the hydrogels were characterized using a scanning electron microscope (SEM, EVO 18, Zeiss, Oberkochen, Germany).

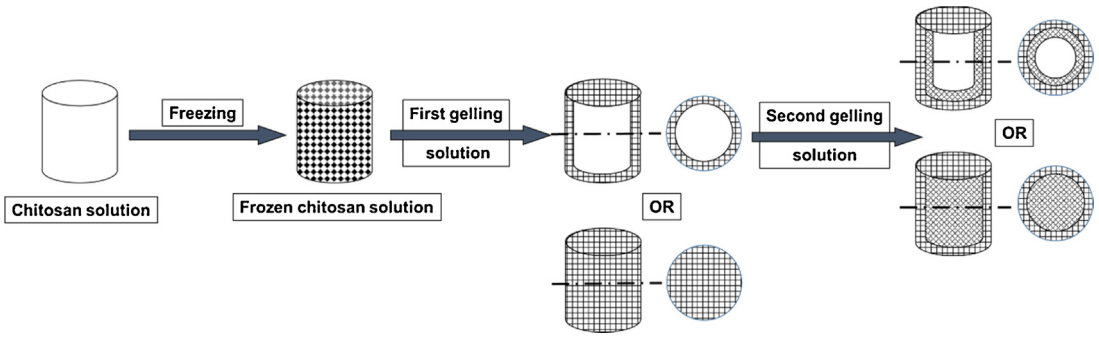

Scheme 1. Schematic illustration of the fabrication of chitosan hydrogels with a gradient structure. The chitosan solution was frozen at −20 °C and then immersed in the first gelling solution (TPP + NaCl) at 4 °C for various times. Then, the hydrogel was further treated by a second gelling solution (NaOH) at 23 °C for a defined period.

2.6. Physico-mechanical characterization of chitosan hydrogels

2.6.1. Swelling ratio (R)

The swelling behavior (water uptake) of the chitosan hydrogel were conducted at 37 °C in 1 × PBS (pH = 7.4) for 24 h. The swelling ratio, *R*, was calculated using the following equation:

$$R = (W_S - W_0)/W_0 \times 100\%$$

where, W_0 is the weight of dry hydrogel after lyophilization and W_s is the weight of swollen hydrogel.

2.6.2. Young's modulus (E)

The mechanical properties, i.e., *E*, of the chitosan hydrogel were determined by compression testing at a rate of 5.0 mm/min and a temperature of 23 ± 2 °C, using a universal material testing machine (model 5543A, Instron, Norwood, MA, USA).

2.7. Cytotoxicity assays

The cytotoxicity of the hydrogels was evaluated using hydrogel extracts and L929 fibroblast cells (ATCC, Manassas, VA, USA) following ISO 10993-5:2001 standards. The test hydrogel extract was prepared with amounts of 0.5, 1.0 and 1.5 mg of chitosan in 1 mL of MEM at 37 °C for 24 h. The L-929 cells (ATCC) were cultured at a density of 1×10^5 cells/well in MEM with 10% FBS at 37 °C and 5% CO_2 for 24 h. The culture medium was then removed and replaced with medium containing the extract. After 24 h, 50 μL of MTT solution (1 mg/mL in PBS) was added to each well, and the cells were incubated at 37 °C for 2 h. The optical intensity was then measured at a wavelength of 570 nm using a microplate reader (Model 680, Bio-Rad, USA).

The blank culture medium and 10% DMSO were used as negative and positive controls, respectively. The cytotoxicity of the hydrogel was expressed as % cell viability, which was calculated from the ratio between the number of cells treated with the polymer solutions and that of non-treated cells (control). Four samples formed in the first gelling solution (3 M NaCl + 0.5% TPP, pH = 5.0 for 1 and 24 h) and the second gelling solution (1.0 M NaOH for 1.0 and 10.0 min) after gelling 1 h in the first gelling solution were tested.

3. Results

3.1. Gelation process of the chitosan hydrogel

The chitosan hydrogel was fabricated utilizing sequential gelling, as illustrated in Scheme 1. Chitosan was solubilized in acetic acid solution and frozen to a desired shape. Subsequently, the chitosan hydrogel was formed in the first gelling solution (TPP + NaCl) for a defined period of time and then again in the second gelling solution (NaOH). The structure and properties of the hydrogel could be tuned by modifying the gelation including gelling time and composition of the two gelling solutions.

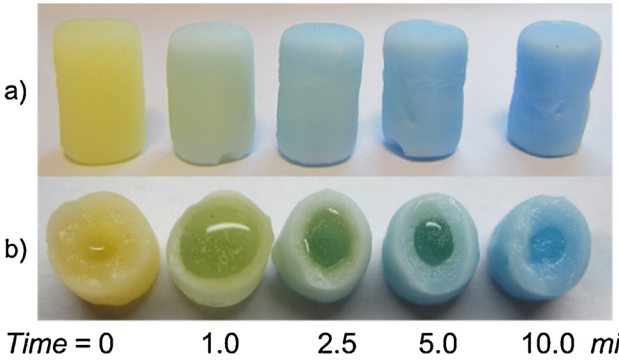

Fig. 2. Digital images showing the chitosan hydrogels formed in the second gelling solution (1.0 M NaOH) at different times (0, 1.0, 2.5, 5.0, and 10.0 min) after gelling 1 h in the first gelling solution (3 M NaCl + 0.5% TPP, pH = 5.0): a) Cylindrical hydrogel; b) Hydrogels after being cut in half. The color of Bromothymol blue changed from yellow to blue when pH >6.0–7.6. (For interpretation of the references to colour in this figure legend, the reader is referred to the web version of this article.)

Fig. 1a shows that chitosan hydrogels formed in the first gelling solution (3 M NaCl + 0.5% TPP, pH 5.0) at different times: 1, 2, 4, 8, and 24 h. After cutting in half, it could be observed that all the solution became gel after 1 h (Fig. 1b). However, the gel on the interior of the sample resulted from the ionic strength-dependent solubility of chitosan. After washing thoroughly with de-ionized water to remove NaCl, this part could be removed completely leaving only the TPP-gelled layer, as shown in Fig. 1c.

Next, after gelling for 1 h in the first gelling solution, the sample was then immersed in the second gelling solution for various times (0, 1.0, 2.5, 5.0, and 10.0 min), as shown in Fig. 2. A color change of the sample from yellow to blue represented that the pH was higher than 6.0–7.6. As illustrated in Fig. 2, the gel layer was thin (blue) and the main interior component was comprised of chitosan solution (yellow) when the gelling time was 1.0 min. With increasing gelling time, the gel layer become thicker and the ratio between solution and gel became smaller. Finally, the solution disappeared and the sample gelled completely at 10 min.

3.2. Gelation rate of the chitosan hydrogel

With the increasing gelling time, the thickness of hydrogel layers increased as shown in Figs. 1c and 2. The gelation rate initially rapid but then slowed. The sample gelled fully in the first gelling solution (3 M NaCl + 0.5% TPP, pH = 5.0) by 24 h, as illustrated in Fig. 3a. In comparison, the second gelling in 1.0 M NaOH was completed in 10 min (Fig. 3b).

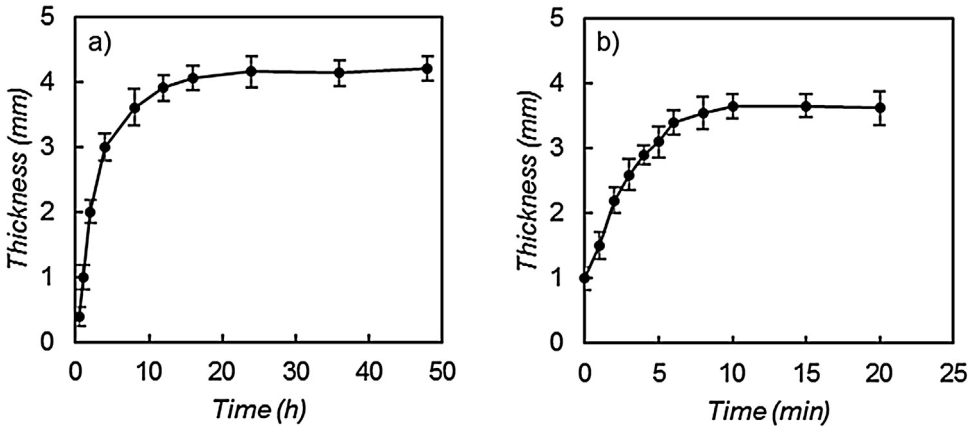

Fig. 3. Change of gel thickness of the hydrogels with time. a) Gelling in the first gelling solution (3 M NaCl + 0.5% TPP, pH = 5.0); b) Further gelling in the second gelling solution (1.0 M NaOH).

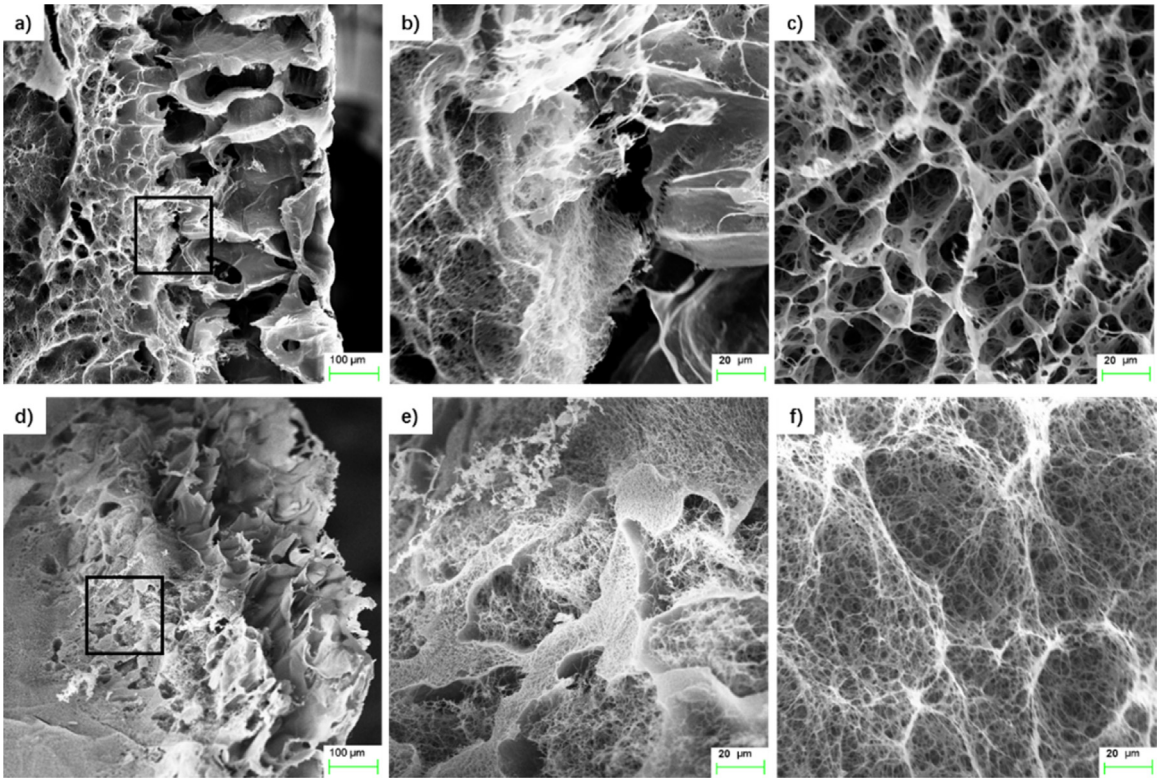

Fig. 4. SEM images (post-lyophilization) of the fracture surfaces of chitosan hydrogels. a), b) (surface) and c) (interior): Gelling in the first gelling solution (3 M NaCl + 0.5% TPP, pH = 5.0) for 1 h; d), e) (surface) and f) (interior): Further gelling in the second gelling solution (1.0 M NaOH) for 10 min.

3.3. Microstructure of the chitosan hydrogel

The fracture surface of the hydrogel was observed using SEM after thorough washing of the sample with de-ionized water and lyophilizing (Annabi et al., 2010). As illustrated in Fig. 4, the hydrogels were mainly composed of three layers. The outer layer comprised a lamellar structure with highly connected pores of 20–50 μm (Fig. 4). At the surface of the frozen chitosan solution, the gelling rate was nearly equal to the melting rate. The chitosan hydrogel formed from the frozen chitosan solution (Fig. 4a). Further internally, the melting rate became gradually higher than the gelling rate. The inside layer gelled from the chitosan solution. The middle layer represented the transition zone (Fig. 4b). When the time was not sufficient for the samples to gel completely, the inside of the sample remained in solution. Fig. 4c shows the internal gel morphology resulting from the lyophilized chitosan solution when the gelling time was 1 h.

After the sample was immersed in 1.0 M NaOH, the inside chitosan solution further gelled because of the increasing pH. At this time, the morphology inside of the sample appeared as a porous structure composed of nano-fibers (Fig. 4f), whereas the morphology at the sample surface changed only slightly (Fig. 4d and e).

3.4. Effect of preparation conditions on the properties of the chitosan hydrogel

As shown in Fig. 5, the properties of the chitosan hydrogel were affected by the first gelation (gelling time, pH, and composition). In particular, the post-treatment methods influenced the properties of the sample. Either de-ionized water or 1 × PBS (pH

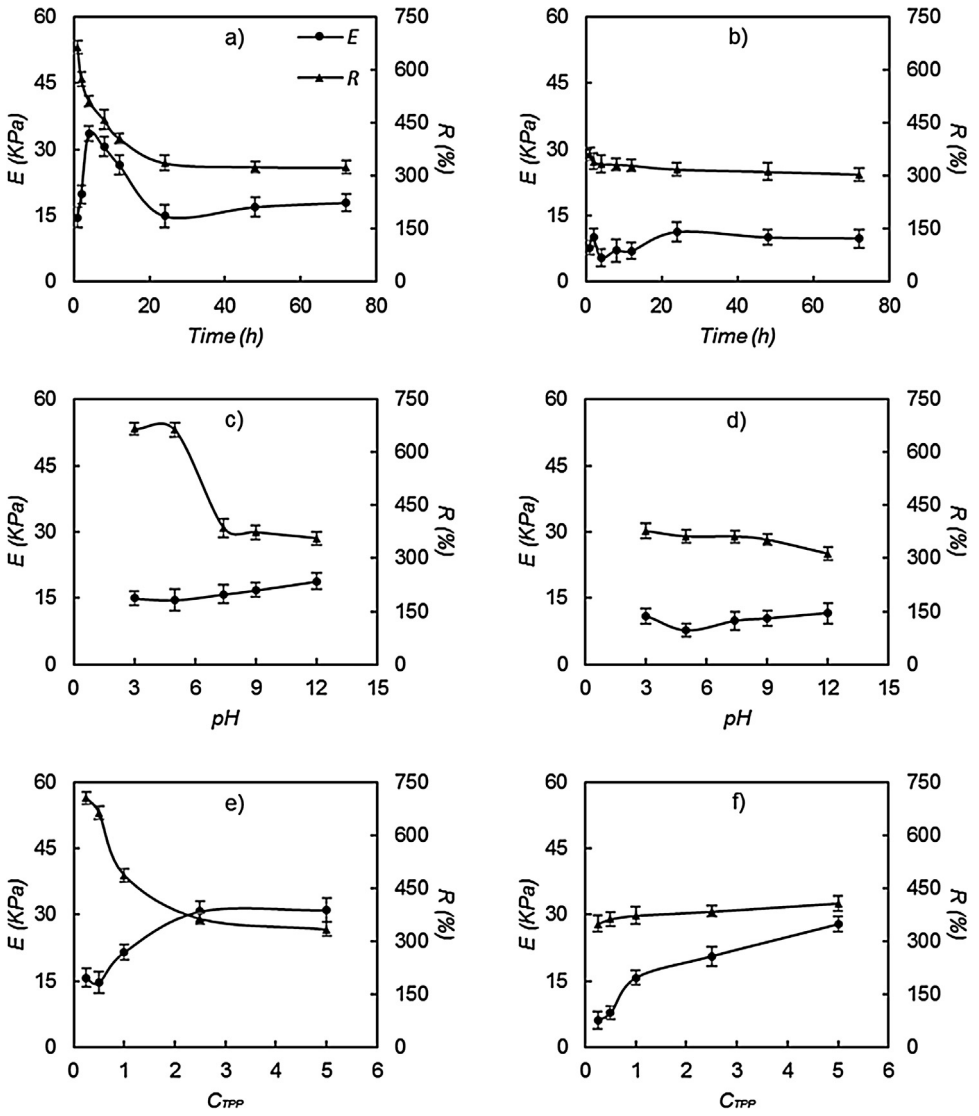

Fig. 5. Effects of the preparation conditions on Swelling ratio (*R*) and Young's modulus (*E*) of chitosan hydrogels in the first gelling solution (3 M NaCl + 0.5% TPP). a) and b) Gelling time (*Time*); c) & d) *pH* of the gelling solution; e) & f) concentration of TPP in the gelling solution (C_{TPP}). a), c), and e): samples in de-ionized water; b), d), and f): samples in 1 × PBS (pH 7.4).

7.4) was used to treat the sample after gelling in order to mimic pseudo-physiological conditions. It was considered that 1 × PBS would further neutralize the uncross-linked chitosan. As shown in Fig. 5, both *E* and *R* were lower in samples treated with 1 × PBS than in de-ionized water.

With increasing gelling time, *E* initially increased and then gradually decreased, eventually remaining constant. In comparison, *R* decreased with increasing gelling time and then also remained constant (Fig. 5a & b). In addition, the compression stress-strain curve showed that the sample would eventually rupture when the gelling time was lower than 24 h (Fig. 6).

As shown in Fig. 5c & d, *E* was higher and *R* was lower when the pH of the gelling solution was higher than 6.3. The concentration of the cross-linker (C_{TPP}) also influenced *E* and *R* values. With increasing C_{TPP}, *E* increased and *R* decreased because of increasing cross-linking density and thickness of the cross-linking layer (Fig. 5e & f).

The second gelation exerted a further influence on the properties of the chitosan hydrogel. After treatment in the first gelling solution for 1 h, the sample was then further treated by NaOH with different times and concentrations. We found that *E* increased and *R*

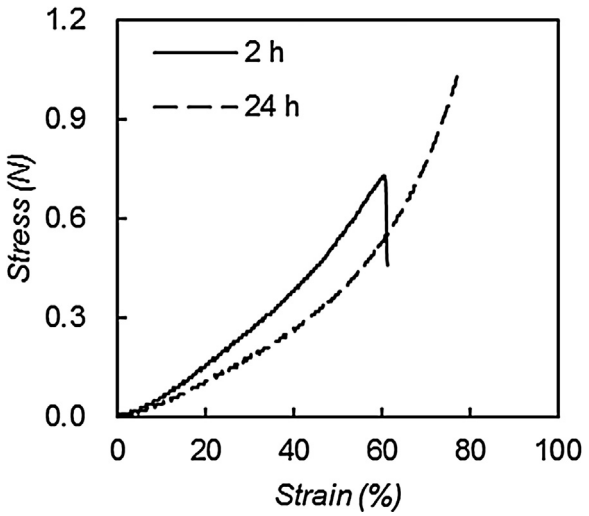

Fig. 6. Compressive stress-strain curves of hydrogels prepared in the first gelling solution (3 M NaCl + 0.5% TPP) at 2 and 24 h.

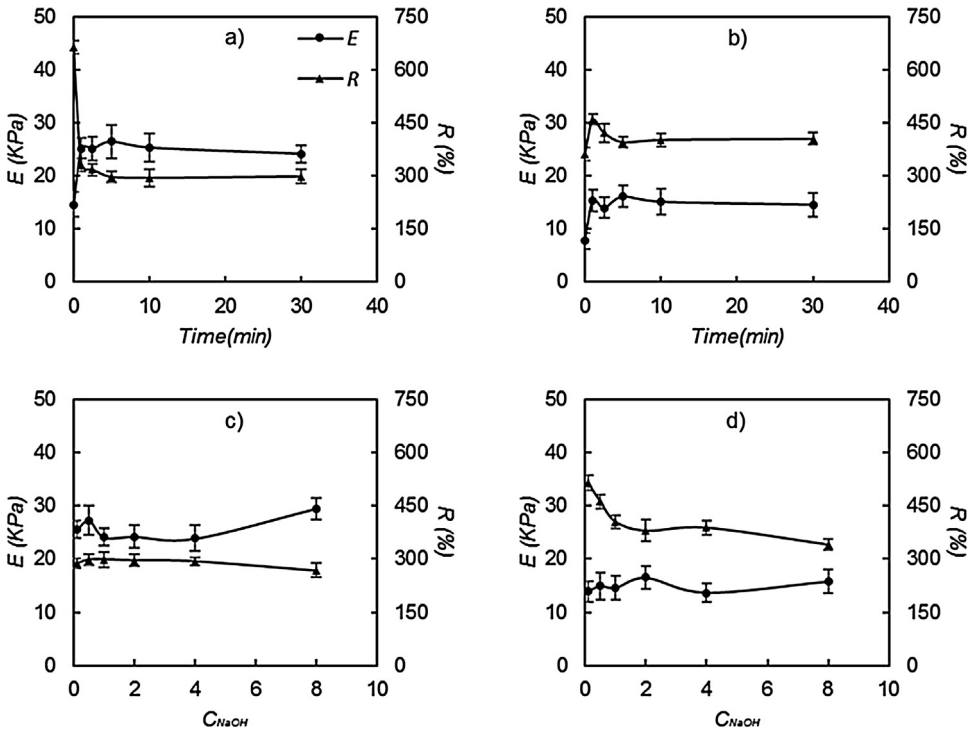

Fig. 7. Effects of preparation conditions on Swelling ratio (R) and Young's modulus (*E*) of chitosan hydrogels in the second gelling solution after 1 h in the first gelling solution. a) and b): Gelling time (*Time*) in 1.0 M NaOH; c) and d): concentration of NaOH solution (C_{NaOH}). a) and c): gelling directly; b) & d): gelling after treatment with de-ionized water.

decreased substantively consequent to the second gelling (Fig. 7). In comparison, *R* and *E* exhibited only minimal change with the increasing gelling time and NaOH concentration (Fig. 7c). Under these conditions, the inner gel resulted from the NaCl-chitosan gelation.

Conversely, neither *R* nor *E* demonstrated marked change as compared with samples not subjected to a second gelling procedure when the samples were first treated with de-ionized water prior to the second gelling (Fig. 7b & d). The morphology illustrated that separated layers formed under this preparation condition. The inner layer gelled from the chitosan solution directly; in contrast to the values obtained from direct gelling, *R* was higher and *E* was lower (Fig. 7a & b, c & d).

3.5. Comparison of the chitosan hydrogel with other preparation conditions

The chitosan hydrogels that fabricated by other conditions as TPP, NaCl + TPP, NaOH and NaCl + NaOH was also prepared as a control. Although the bulk chitosan hydrogel could be fabricated in these conditions, the properties were different, as shown in Fig. 8. Furthermore, the hydrogels from 0.5% TPP and 1.0 M NaOH had a hollow structure. The hydrogel that prepared by 1.0 M NaOH and 3 M NaCl + 1.0 M NaOH would change to liquid in acid environment and limited its application.

3.6. In vitro *cytotoxicity of chitosan hydrogel*

The cytotoxicity of the chitosan hydrogel was determined using an MTT assay. As illustrated in Fig. 9, the hydrogel formed in the first gelling solution (3 M NaCl + 0.5% TPP, pH = 5.0) for 1 h showed only slight cytotoxicity because of the weak acid of uncross-linking chitosan solution inside the sample. The other three samples demonstrate cytocompatible for fibroblast cells.

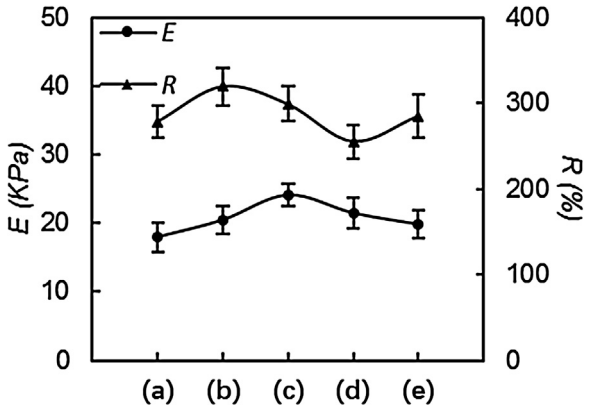

Fig. 8. Young's modulus (*E*) and Swelling ratio (R) of chitosan hydrogels at different gelling solution. a): 0.5% TPP; b): 3 M NaCl + 0.5% TPP; c): 3 M NaCl + 0.5% TPP and 1.0 M NaOH; d): 1.0 M NaOH; e): 3 M NaCl + 1.0 M NaOH.

4. Discussion

Polysaccharide-based hydrogels are useful for numerous applications from food and cosmetic processing to drug delivery and tissue engineering (Drury & Mooney, 2003). Of these, gradient hydrogels have attracted considerable attention because of their potential to mimic the gradient structure of natural tissue.

In this study, chitosan hydrogels with gradient structure were designed and fabricated via a step-by-step gelation. In the first step, the chitosan solution was frozen to an expected shape and then gelled with TPP and NaCl from the surface of the sample. The cross-linking conditions could be tuned to control the structure and morphology of the outer gelled layers. Conversely, the interior of the sample remained in a state of solution at some gelling conditions. In the second step, the inner chitosan solution was further gelled using NaOH by increasing the pH of the chitosan solution.

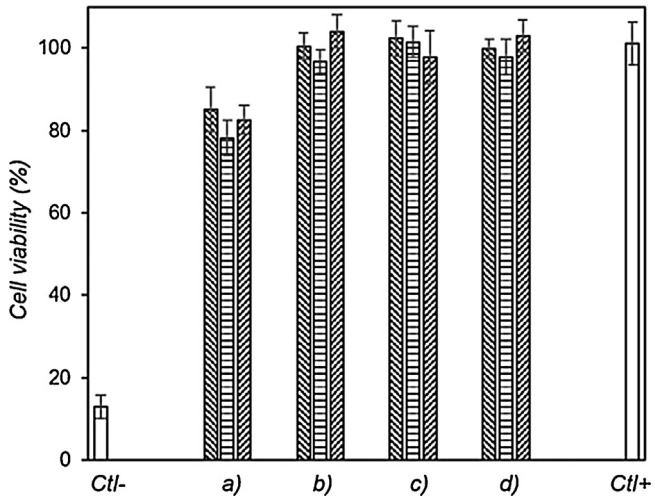

Fig. 9. Viability of L929 fibroblasts exposed to extracts during incubation with various chitosan hydrogels at different concentrations (0.5, 1.0 and 1.5 mg/mL). Ctl−, 10% DMSO; Ctl+, medium culture; a) & b): Hydrogels formed in the first gelling solution (3 M NaCl + 0.5% TPP, pH = 5.0 for 1 and 24 h; c) & d): Hydrogels formed the second gelling solution (1.0 M NaOH) for 1.0 and 10.0 min after gelling 1 h in the first gelling solution.

During this process, the gel structure could also be tuned by the gelling time and the concentration of NaOH. Finally, these processes resulted in the fabrication of a hydrogel with three layers. The outer layer was formed by TPP-gelling, the middle layer was from NaOH-gelling, and the inner layer represented chitosan solution. The hydrogel could also be controlled to generate a double-layered (TPP-gelling/chitosan solution or TPP-gelling/NaOH-gelling) or a single layer (TPP-gelling) structure by varying the different gelationes. The high ionic strength from NaCl played a key role in the fabrication process.

In the first gelling step, NaCl was used to maintain the shape of frozen samples and TPP was used to gelling the chitosan. The structure and properties of the hydrogels were affected by gelling time, pH, and composition of the first gelling solution. Chitosan is solubilized by dilute acids by the protonation of amine groups ($-NH_2$ to $-NH_3^+$), which causes electrostatic repulsion between the polymer chains, rendering the corresponding chitosan salt soluble. Although TPP has often been used as an ionic gelling agent for chitosan, a flocculent precipitate occurred when TPP was blended directly with the chitosan solution. To reduce the possibly of chitosan precipitate and fabricate a hydrogel scaffold with a defined shape, we utilized a freezing process to prepare the sample prior to TPP gelling. During the gelation, the frozen samples began to melt in the gelling solution because of its high temperature, while simultaneously TPP began to gel the chitosan solution. However, if the TPP gelling rate was not fast enough to form a strong outer layer, which was important to maintain the shape of the sample, the gel would deform and even break up into pieces of flocculent precipitate. Therefore, high ionic strength (Cl^-) was used to electronically screen the NH_3^+ and prevent chitosan solubility because of the high diffusion rate of Cl^- into the chitosan solution. Finally, Cl^- was replaced by TPP and the ionic gelling layer could form.

Notably, the structure and properties of the hydrogel could be tuned by modifying the first gelling conditions. When the gelling time was lower than 24 h, a hydrogel with two layers (TPP-gelling layer and chitosan solution layer) formed and the thickness of the gel layer increased with gelling time. *E* was affected by both the outer gel layer and the inner chitosan solution, such that the electrostatic repulsion of the inner chitosan solution enhanced the *E* value to a certain degree. The *E* value decreased immediately to nearly zero when the outer layer ruptured. After 24 h, a hydrogel with only a single layer (TPP-gelling) formed, for which the properties no longer changed with the increasing gelling time. When the pH of the first gelling solution was higher than 6.3, gelling from OH^- neutralization occurred in synchronization with TPP gelling (Bhumkar & Pokharkar, 2006; Mi, Shyu, Lee, & Wong, 2015; Pati, Adhikari, & Dhara, 2011). The increasing TPP concentration also resulted in an increase of thickness and gelling density of the outer gel layer.

In the second gelling step, NaCl assisted NaOH to gel the inner chitosan of the sample. Neutralization of NH_3^+ of the chitosan solution with OH^- leads to the disappearance of ionic repulsion between the polymer chains, which favors physical gelling corresponding to hydrogen bonding, hydrophobic interactions, and crystallite formation (Ilmain, Tanaka, & Kokufuta, 1991). In the current study, two methods were used to gel the samples. In the first, the samples were immersed in NaOH directly without any other treatment. In this case, the inner chitosan solution of the sample remained in the gel state because of the ionic screening of NaCl, wherein OH^- gradually replaced the Cl^- from exterior to the interior of the sample and the gel remained with an uninterrupted morphology. The other method involved immersing the samples in NaOH after three washes with de-ionized water and followed by storage in the rinse solution for 24 h. In this case, the inner chitosan solution of the sample transitioned into the solution state from the gel state because the NaCl was completely washed out by water and a flocculent precipitate formed in NaOH. Consequently, their mechanical properties were lower than those of the hydrogels neutralized directly after the first gelling solution.

5. Conclusions

A step-by-step gelling method was developed to prepare gradient chitosan hydrogel by TPP, NaOH and NaCl. Ionic-dependent solubility of chitosan played a key role in the fabrication process. The structure and properties of the resultant chitosan hydrogel could be tuned by the gelling conditions. Hydrogels with single, double, and triple layers were fabricated by using the different gelling conditions. Cell viability experiments showed cytocompatibility for fibroblast cells. They could be further used as scaffold to mimic the gradient structure of natural tissues

Acknowledgement

The work was supported by the National Natural Science Foundation of China (grant number 81200814).

References

Abd-Allah, H., Kamel, A. O., & Sammour, O. A. (2016). Injectable long acting chitosan/tripolyphosphate microspheres for the intra-articular delivery of lornoxicam: Optimization and in vivo evaluation. *Carbohydrate Polymers*, *149*, 263–273.

Agnihotri, S. A., Mallikarjuna, N. N., & Aminabhavi, T. M. (2004). Recent advances on chitosan-based micro-and nanoparticles in drug delivery. *Journal of Controlled Release*, *100*(1), 5–28.

Anitha, A., Maya, S., Deepa, N., Chennazhi, K. P., Nair, S. V., Tamura, H., et al. (2011). Efficient water soluble O-carboxymethyl chitosan nanocarrier for the delivery of curcumin to cancer cells. *Carbohydrate Polymers*, *83*(2), 452–461.

Annabi, N., Nichol, J. W., Zhong, X., Ji, C., Koshy, S., Khademhosseini, A., et al. (2010). Controlling the porosity and microarchitecture of hydrogels for tissue engineering. *Tissue Engineering Part B Reviews*, *16*(4), 371–383.

Berger, J., Reist, M., Mayer, J. M., Felt, O., & Gurny, R. (2004). Structure and interactions in chitosan hydrogels formed by complexation or aggregation for biomedical applications. *European Journal of Pharmaceutics and Biopharmaceutics*, *57*(1), 35–52.

Bhattarai, N., Gunn, J., & Zhang, M. (2010). Chitosan-based hydrogels for controlled, localized drug delivery. *Advanced Drug Delivery Reviews*, *62*(1), 83–99.

Bhumkar, D. R., & Pokharkar, V. B. (2006). Studies on effect of pH on cross-linking of chitosan with sodium tripolyphosphate: A technical note. *AAPS PharmSciTech*, *7*(2), E138–E143.

Brugnerotto, J., Lizardi, J., Goycoolea, F., Argüelles-Monal, W., Desbrieres, J., & Rinaudo, M. (2001). An infrared investigation in relation with chitin and chitosan characterization. *Polymer*, *42*(8), 3569–3580.
Burdick, J. A., Chung, C., & Jia, X. (2005). Controlled degradation and mechanical behavior of photopolymerized hyaluronic acid networks. *Biomacromolecules*, *6*(1), 386–391.
Chatterjee, K., Sun, L., Chow, L. C., Young, M. F., & Simon, C. G., Jr. (2010). Combinatorial screening of osteoblast response to 3D calcium phosphate/poly(ε-caprolactone) scaffolds using gradients and arrays. *Biomaterials*, *32*(5), 1361–1369.
Dash, M., Chiellini, F., Ottenbrite, R., & Chiellini, E. (2011). Chitosan—A versatile semi-synthetic polymer in biomedical applications. *Progress in Polymer Science*, *36*(8), 981–1014.
Domard, A. (2011). A perspective on 30 years research on chitin and chitosan. *Carbohydrate Polymers*, *84*(2), 696–703.
Drury, J. L., & Mooney, D. J. (2003). Hydrogels for tissue engineering: Scaffold design variables and applications. *Biomaterials*, *24*(24), 4337–4351.
Geckil, H., Xu, F., Zhang, X., Moon, S., & Demirci, U. (2010). Engineering hydrogels as extracellular matrix mimics. *Nanomedicine*, *5*(3), 469–484.
Ho, M.-H., Kuo, P.-Y., Hsieh, H.-J., Hsien, T.-Y., Hou, L.-T., Lai, J.-Y., et al. (2004). Preparation of porous scaffolds by using freeze-extraction and freeze-gelation methods. *Biomaterials*, *25*(1), 129–138.
Hsieh, C.-Y., Tsai, S.-P., Ho, M.-H., Wang, D.-M., Liu, C.-E., Hsieh, C.-H., et al. (2007). Analysis of freeze-gelation and cross-linking processes for preparing porous chitosan scaffolds. *Carbohydrate Polymers*, *67*(1), 124–132.
Hui, Y. Z., Ling, J. J., Pei, P. C., Li, J. B., & Xi, G. C. (2015). Glycerophosphate-based chitosan thermosensitive hydrogels and their biomedical applications. *Carbohydrate Polymers*, *117C*(117C), 524–536.
Ilmain, F., Tanaka, T., & Kokufuta, E. (1991). Volume transition in a gel driven by hydrogen bonding. *Nature*, *349*(6308), 400–401.
Jeon, O., Alt, D. S., Linderman, S. W., & Alsberg, E. (2013). Biochemical and physical signal gradients in hydrogels to control stem cell behavior. *Advanced Materials*, *25*(44), 6366–6372.
Jin, L., Zeng, X., Liu, M., & He, N. (2013). Chitosan/polylactic acid/tripolyphosphate nanocapsules for encapsulation of water-insoluble drugs: in vitro drug release and cytotoxicity. *Science of Advanced Materials*, *5*(12), 2053–2057.
Karpiak, J. V., Ner, Y., & Almutairi, A. (2012). Density gradient multilayer polymerization for creating complex tissue. *Advanced Materials*, *24*(11), 1466–1470.
Kim, T. H., Dan, B. A., Oh, S. H., Min, K. K., Song, H. H., & Jin, H. L. (2015). Creating stiffness gradient polyvinyl alcohol hydrogel using a simple gradual freezing–thawing method to investigate stem cell differentiation behaviors. *Biomaterials*, *40*, 51–60.
Ladet, S., David, L., & Domard, A. (2008). Multi-membrane hydrogels. *Nature*, *452*(7183), 76–79.
Levengood, S. L., & Zhang, M. (2014). Chitosan-based scaffolds for bone tissue engineering. *Journal of Materials Chemistry B Materials for Biology & Medicine*, *2*(21), 3161–3184.
Levingstone, T. J., Matsiko, A., Dickson, G. R., O'Brien, F. J., & Gleeson, J. P. (2014). A biomimetic multi-layered collagen-based scaffold for osteochondral repair. *Acta Biomaterialia*, *10*(5), 1996–2004.
Mahadik, B. P., Wheeler, T. D., Skertich, L. J., Kenis, P. J. A., & Harley, B. A. C. (2014). Microfluidic generation of gradient hydrogels to modulate hematopoietic stem cell culture environment. *Advanced Healthcare Materials*, *3*(3), 449–458.
Mi, F. L., Shyu, S. S., Lee, S. T., & Wong, T. B. (2015). Kinetic study of chitosan-tripolyphosphate complex reaction and acid-resistive properties of the chitosan-tripolyphosphate gel beads prepared by in-liquid curing method. *Journal of Polymer Science Part B Polymer Physics*, *37*(37), 1551–1564.
Mohan, N., Dormer, N. H., Caldwell, K. L., Key, V. H., Berkland, C. J., & Detamore, M. S. (2011). Continuous gradients of material composition and growth factors for effective regeneration of the osteochondral interface. *Tissue Engineering Part A*, *17*(21–22), 2845–2855.
Montembault, A., Viton, C., & Domard, A. (2005). Rheometric study of the gelation of chitosan in aqueous solution without cross-linking agent. *Biomacromolecules*, *6*(2), 653–662.
Nie, J., Wang, Z., Zhang, K., & Hu, Q. (2015). Biomimetic multi-layered hollow chitosan tripolyphosphate rod with excellent mechanical performance. *RSC Advances*, *5*(47), 37346–37352.
O'Brien, F. J. (2011). Biomaterials & scaffolds for tissue engineering. *Materials Today*, *14*(3), 88–95.
Pati, F., Adhikari, B., & Dhara, S. (2011). Development of chitosan-tripolyphosphate fibers through pH dependent ionotropic gelation. *Carbohydrate Research*, *346*(16), 2582–2588.
Pedron, S., Becka, E., & Harley, B. A. (2015). Hydrogels: Spatially gradated hydrogel platform as a 3D engineered tumor microenvironment. *Advanced Materials*, *27*(9), 1567–1572.
Rampino, A., Borgogna, M., Blasi, P., Bellich, B., & Cesàro, A. (2013). Chitosan nanoparticles: Preparation, size evolution and stability. *International Journal of Pharmaceutics*, *455*(1–2), 219–228.
Sashiwa, H., & Aiba, S.-i. (2004). Chemically modified chitin and chitosan as biomaterials. *Progress in Polymer Science*, *29*(9), 887–908.
Seidi, A., Ramalingam, M., Elloumi-Hannachi, I., Ostrovidov, S., & Khademhosseini, A. (2011). Gradient biomaterials for soft-to-hard interface tissue engineering. *Acta Biomaterialia*, *7*(4), 1441–1451.
Silva, A. K., Juenet, M., Meddahi-Pellé, A., & Letourneur, D. (2015). Polysaccharide-based strategies for heart tissue engineering. *Carbohydrate Polymers*, *116*, 267–277.
Slaughter, B. V., Khurshid, S. S., Fisher, O. Z., Khademhosseini, A., & Peppas, N. A. (2009). Hydrogels in regenerative medicine. *Advanced Materials*, *21*(32–33), 3307–3329.
Sobral, J. M., Caridade, S. G., Rui, A. S., Mano, J. F., & Rui, L. R. (2011). Three-dimensional plotted scaffolds with controlled pore size gradients: Effect of scaffold geometry on mechanical performance and cell seeding efficiency. *Acta Biomaterialia*, *7*(3), 1009–1018.
Tan, Y., Wu, R., Li, H., Ren, W., Du, J., Xu, S., et al. (2015). Electric field-induced gradient strength in nanocomposite hydrogel through gradient crosslinking of clay. *Journal of Materials Chemistry B*, *3*(21), 4426–4430.
Zhang, Y., Yang, B., Zhang, X., Xu, L., Tao, L., Li, S., et al. (2012). A magnetic self-healing hydrogel. *Chemical Communications*, *48*(74), 9305–9307.